A new sensor with increased lifetime based on a mixed diazonium thick film/gold nanoparticles interface for Hg(II) trace detection

Fatma Fezai, Childérick Séverac, Pierre Gros, Martine Meireles, David Evrard

A New Sensor with Increased Lifetime Based on a Mixed Diazonium Thick Film/Gold Nanoparticles Interface for Hg(II) Trace Detection

Fatma Fezai,[a] Childérick Séverac,[b] Pierre Gros,[a] Martine Meireles,[a] and David Evrard*[a]

Abstract: This work describes a novel strategy for surface functionalization, the aim of which is to significantly increase the lifetime of an electrochemical sensor dedicated to Hg(II) trace determination. In order to tailor stable mixed organic/inorganic interfaces, gold nanoparticles were electrodeposited onto a glassy carbon electrode previously functionalized by a thick 4-thiophenol diazonium film, which affords a good anchoring to the nanoparticles. AFM and FEG-SEM were used to characterize the film thickness and the nanoparticles average size and density, respectively. By using square wave anodic stripping voltammetry, the sensor exhibited a linear response between 1 and 10 nM Hg(II) and a normalized sensitivity 0.03 μA nM^{-1} min^{-1}. Compared to previous works, the storage lifetime of the interface was at least three times longer, being more than three weeks.

Keywords: Hg(II) electrochemical sensor · Gold nanoparticles electrodeposition · thick diazonium film · increased sensor lifetime

Trace metal elements determination is one of the most critical concern with respect to environmental sustainability [1] and human health [2]. Electrochemistry is particularly well-suited to face this challenge and build sensors which satisfy all the requirements to operate directly in natural media and to reach trace concentration range [3]. One of the key features is actually electrode surface functionalization, which is expected to afford all the desired properties [4]. In the course of interface tailoring, tremendous attention has been paid on selectivity and sensitivity [5]. On the contrary, the issue of sensor lifetime is rarely addressed in the literature.

Considering Hg(II) as the priority target element, we have previously developed an electrochemical sensor based on gold nanoparticle-functionalized glassy carbon electrode (GC/AuNPs) [6]. Using square wave anodic stripping voltammetry (SWASV), the GC/AuNPs electrode exhibited a linear response in the nM range associated to a normalized sensitivity of 0.60 μA nM^{-1} min^{-1} and a limit of detection (LOD) of 80 pM [7]. Natural water analysis was successfully conducted and a value as low as 19±3 pM was found by increasing preconcentration duration [7]. However, the GC/AuNPs interface failed stability tests: an adequate detection of a given Hg(II) amount was possible only over a few consecutive days. In order to fix this issue, a mixed organic/inorganic functionalization has been envisaged by combining diazonium salts and AuNPs. To achieve such mixed organic/inorganic interface, the AuNPs were first prepared via colloidal route and subsequently drop-casted onto a thick diazonium film [8]. However, no significant improvement of the interface stability vs time has been evidenced in this latter work. Alternative strategies have been reported in the literature to build mixed organic/inorganic interfaces. One of them consists in the immobilization of metallic cations on the top of an aryl monolayer-functionalized surface and subsequent cations reduction [9]. In these latter works, no information was provided upon the interface stability vs time. The diazotization of aminated NPs followed by diazonium reduction and grafting has been also reported [10]. In this case, a pretty good stability was reported, but this strategy is expected to be unsuitable for trace metal elements determination, due to the presence of the capping ligands on the NPs surface, which may hamper metal accumulation during the preconcentration step. From this point of view, NPs electrodeposition offers the advantage of providing ligand-free NPs. However, NPs electrodeposition on aryldiazonium has been rarely described in the literature. Mirkhalaf et al. have electrodeposited AuNPs on a submonolayer, inhomogeneous 4-nitrosophenyl film [11]. González et al. have performed the reduction of $HAuCl_4$ on 4-nitrobenzenediazonium-functionalized carbon substrates by cyclic voltammetry [12]. It is worth noting that in these last two works the film growth was controlled down to a monolayer by using a radical scavenger. Indeed, such a precaution was taken because multilayer, thick aryldiazonium films are well-known to

[a] F. Fezai, P. Gros, M. Meireles, D. Evrard
Laboratoire de Génie Chimique
Université de Toulouse, CNRS, INPT, UPS
Toulouse, France
E-mail: evrard@chimie.ups-tlse.fr
[b] C. Séverac
ITAV
Université de Toulouse, CNRS
Toulouse, France

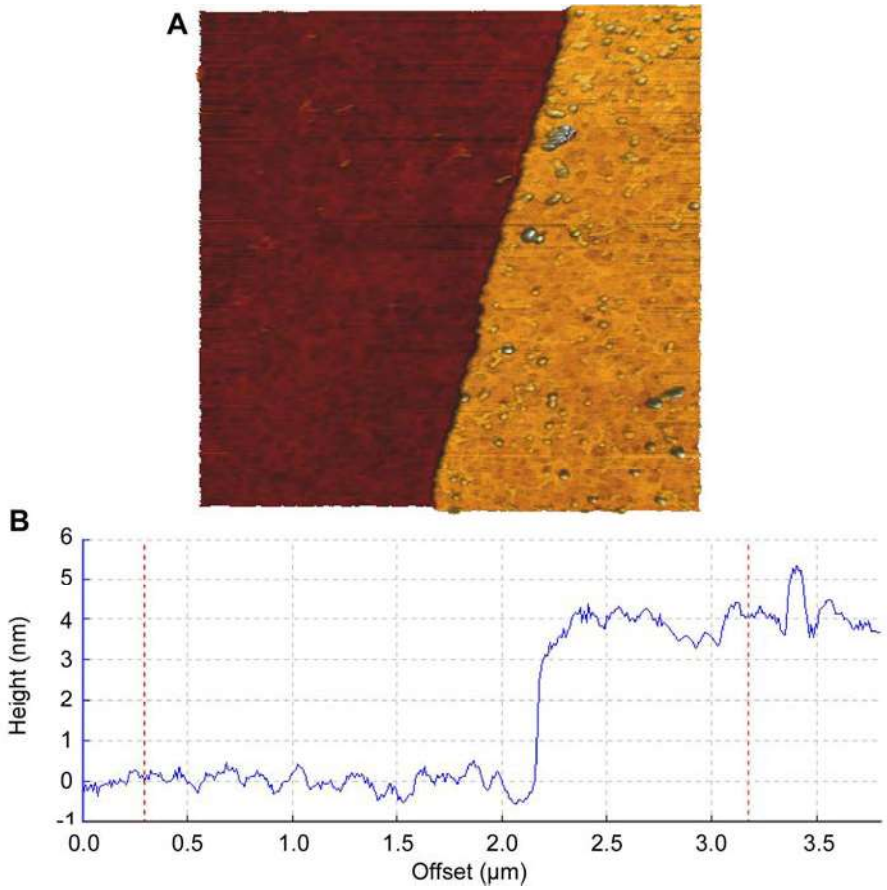

Fig. 1. (A) $5 \times 5\ \mu m^2$ AFM micrograph of $GC/SH_{(CPE)}$. (B) Thickness profile of the organic film.

result in a strong barrier effect [13], thus severely hampering the electrodeposition process. The case of thick aryldiazonium films should however be considered since such thick structures may maximize interactions with AuNPs and thus improve their stability. Here we report for the first time the electrodeposition of AuNPs onto a thick diazonium film and the resulting increase in sensor lifetime brought by this mixed organic/inorganic interface.

The cyclic voltammogram (CV) recorded on a GC electrode in a 0.1 M HCl solution containing 1.5 mM 4-thiophenol diazonium exhibited a large reduction peak at −0.3 V (not shown), which corresponds to the diazonium reduction and subsequent grafting onto GC surface as previously reported by our group [8]. In order to produce multilayered, self-inhibiting films, GC functionalization was achieved by constant potential electrolysis (CPE) at −0.5 V for 300 s. Figure 1A shows an AFM micrograph of the resulting functionalized $GC/SH_{(CPE)}$ electrode. A thick and almost homogeneous film was observed, with some "mushroom-like" structures. The thickness of the film was found to be 4 nm (Figure 1B), which compares favorably with previous results from our group [8].

The barrier effect [13] of the film was evaluated by recording CVs using 5 mM ferricyanide on bare GC and on $GC/SH_{(CPE)}$ (Figure 2A). On bare GC (black, solid line), the classical one-electron quasi-reversible ($\Delta E_p =$ 220 mV) system of ferricyanide centered at 0.18 V was observed [13b, 16]. On the contrary, on $GC/SH_{(CPE)}$ (red, dashed line) this latter signal was almost totally suppressed, as the consequence of a strong barrier effect of the SH-bearing film [8]. For the sake of comparison, CVs were also recorded in the same conditions using $Ru(NH_3)_6^{3+}$ (Figure 2B). On bare GC, this latter redox probe exhibited a fast, reversible ($\Delta E_p = 98$ mV) system located at −0.18 V. On $GC/SH_{(CPE)}$, contrary to what was observed with ferricyanide, a redox system was still noticed. This is consistent with the fact that $Ru(NH_3)_6^{3+}$ redox process occurs via an outer-sphere mechanism, which makes it much less sensitive to surface changes than ferricyanide, the reduction process of which mainly occurs via an inner-sphere mechanism. However, the redox system of $Ru(NH_3)_6^{3+}$ was much slower on $GC/SH_{(CPE)}$ than on bare GC, thus definitely confirming the presence of the organic film onto the electrode, and its influence on the redox kinetics.

In order to achieve further functionalization of the $GC/SH_{(CPE)}$ electrode, another CVs were recorded in a 0.1 M $NaNO_3$ solution containing 0.25 mM $HAuCl_4$ (Figure 3A). On the first forward scan (red, dashed line) a large cathodic peak was observed at 0.12 V, which is consistent with Au(III) reduction into Au(0) and subse-

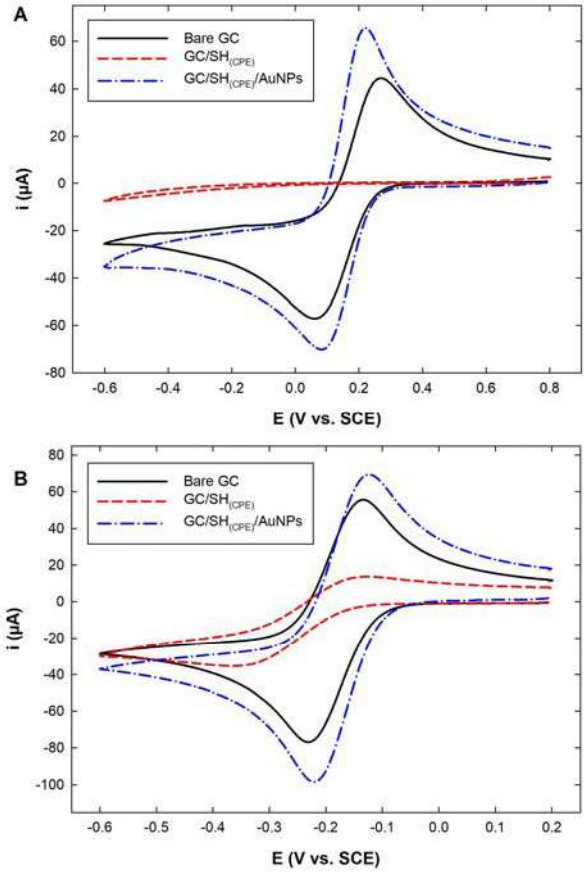

Fig. 2. CVs recorded in a 0.1 M KNO_3 solution containing (A) 5 mM ferricyanide or (B) 5 mM $Ru(NH_3)_6^{3+}$ on different electrodes. Scan rate: 100 mV s^{-1}.

quent AuNPs deposition onto $GC/SH_{(CPE)}$. On the first backward scan, a current crossover occurred around 0.37 V, which corresponds to the thermodynamically favored deposition of Au on previously formed AuNPs [17], thus proving the nanoparticles electrodeposition to be effective despite the presence of a thick organic film. On the second scan (blue, dashed-dotted line), a peak located at 0.61 V was recorded, which corresponds to the reduction of Au(III) on the AuNPs previously formed during the first scan. Regarding this electrodeposition process which appears to be quite unexpected on a thick, insulating diazonium film, one may carefully examine the CV of ferricyanide on $GC/SH_{(CPE)}$ (Figure 2A): the corresponding redox signal is actually very small, but not totally suppressed, probably because of the presence of some pinholes or defects in the film [18]. Thus, the formation of the first nuclei may be due to Au(III) reduction which occurs via these pinholes. One has also to keep in mind that the organic film bears SH groups, and that Au exhibits a strong affinity for Sulphur atom: this may also help at the electrodeposition process, by favoring the Au(III) approach to the electrode surface. It is worth noting that Au(III) reduction is slower and more

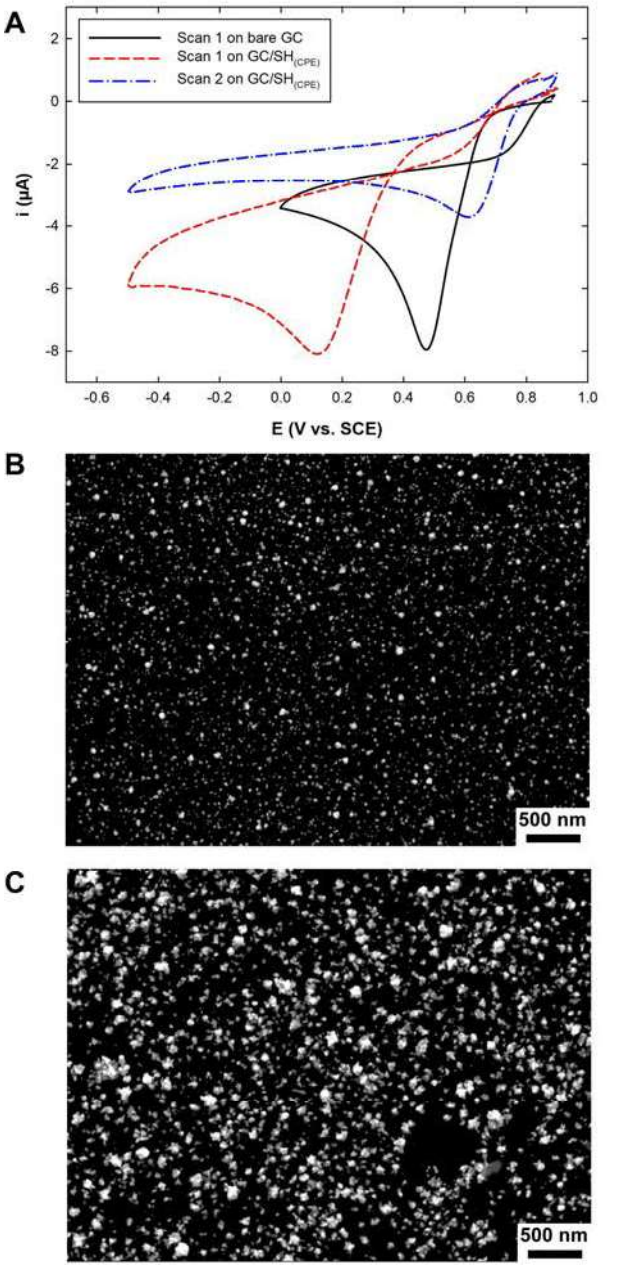

Fig. 3. (A) CVs recorded in a deaerated 0.1 M $NaNO_3$ solution containing 0.25 mM $HAuCl_4$ on different electrodes. Scan rate: 50 mV s^{-1}. (B, C) FEG-SEM micrographs of $GC/SH_{(CPE)}$/AuNPs with AuNPs electrodeposited by CPE at 0.05 V for (B) 300 s or (C) 600 s.

difficult on $GC/SH_{(CPE)}$ compared to bare GC, for which a narrow peak is observed at a potential around 360 mV higher, ca. 0.48 V (Figure 3A, solid, black line), as previously reported [6].

CVs recorded in a 0.1 M KNO_3 solution containing 5 mM ferricyanide or $Ru(NH_3)_6^{3+}$ on $GC/SH_{(CPE)}$/AuNPs (Figure 2, blue, dashed-dotted lines) exhibited the quasi-reversible and reversible systems of the probes, respec-

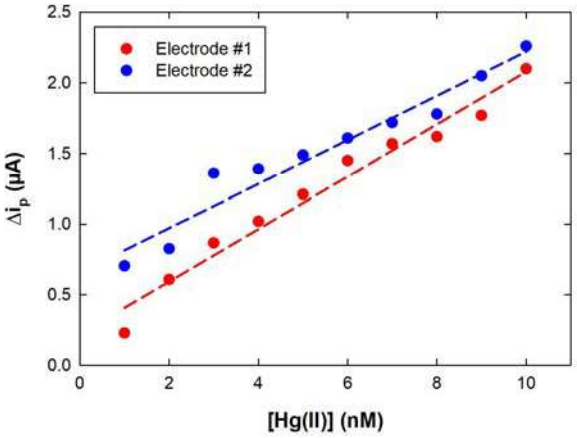

Fig. 4. Calibration curves obtained by SWASV on two different GC/SH/AuNPs electrodes in a deaerated 0.01 M HCl with increasing amounts of Hg(II).

tively, the current of which was enhanced in both cases due to the increase in active surface area afforded by the NPs. Moreover, the ΔE_p decreased down to 140 mV and 95 mV, respectively, as the consequence of an electrocatalytic process. All these results showed that the electron transfer throughout the film was restored after AuNPs electrodeposition, confirming that Au(III) reduction is effective on $GC/SH_{(CPE)}$.

To definitely prove that AuNPs electrodeposition was efficient even on the most blocking $GC/SH_{(CPE)}$ surfaces, FEG-SEM was recorded on several interfaces (Figure 3B, C). When AuNPs were prepared by CPE at 0.05 V for 300 s ($GC/SH_{(CPE)}/AuNPs_{(CPE)}$), a quite homogeneous deposit was obtained in terms of average diameter, ca. 27 ± 3 nm (Figure 3B). However, a size distribution of NPs was observed, contrary to what we previously reported on bare GC [6b]. This could be due to different electronic environments in the film which locally modify the potential experienced by Au(III) during the reduction process. The corresponding NPs density was 158 NPs/µm^2. When electrodeposition duration was increased up to 600 s (Figure 3C), large structures (ca. 63 ± 6 nm) were obtained with a much lower density (ca. 63 NPs/µm^2). These structures resulted from the coalescence or aggregation of AuNPs, in a similar trend to previously reported observations [6b]. These results, which compare favorably with our previous works [6], suggest that once started, the electrodeposition process globally occurs following the same trend whether the organic film is present or not.

The as-prepared $GC/SH_{(CPE)}/AuNPs_{(CPE)}$ electrode was tested with respect to Hg(II) trace determination. Increasing amounts of Hg(II) were successively added to a 0.01 M HCl solution and SWASVs were recorded. Figure 4 shows the response obtained using two different $GC/SH_{(CPE)}/AuNPs_{(CPE)}$ electrodes prepared using the same protocol.

In both cases a linear trend was observed in the range 1–10 nM Hg(II), associated to a normalized sensitivity of 0.03 µA nM^{-1} min^{-1}. This latter value is one order of magnitude lower than that previously reported by our group using GC/AuNPs (ca. 0.23 and 0.60 µA nM^{-1} min^{-1}) [6b,7] and two orders of magnitude lower than the value we recently reported using AuNPs prepared via colloidal route and drop-casted onto GC/SH electrode (ca. 3.94 µA nM^{-1} min^{-1}) [8]. This confirms that electrogenerated AuNPs are much less reactive than chemically-prepared ones. Moreover, no sensitivity enhancement was brought by the presence of the SH diazonium film, contrary to what was observed in our previous report [8]. The $GC/SH_{(CPE)}/AuNPs_{(CPE)}$ electrodes exhibited good reproducibility, as can be seen from the similarity of both electrodes response.

The critical issue of sensor lifetime was then examined by storing two $GC/SH_{(CPE)}/AuNPs_{(CPE)}$ electrodes in air without any special care for several days, in order to mimic real operating conditions. For the sake of comparison, two GC/AuNPs electrodes were also stored using the same protocol. The evolution of the electrodes response was checked by recording SWASVs in a 0.01 M HCl solution containing 4 nM Hg(II).

Figure 5 (A, B) shows the evolution of the SWASVs recorded on GC/AuNPs and on $GC/SH_{(CPE)}/AuNPs_{(CPE)}$ between the day of preparation of the electrodes (Day #0) and after several days of storage. On GC/AuNPs (Figure 5A), the SWASV recorded at Day #0 exhibited two well-defined peaks located at 0.28 V and 0.56 V, respectively. On the basis of previous studies [6], this latter peak was assigned to Hg(0) reoxidation, whereas the peak located at 0.28 V corresponded to chloride anions desorption, as previously demonstrated by our group [19]. After seven days of storage, dramatic changes were observed on the SWASV recorded on GC/AuNPs. Indeed, the voltammogram exhibited a very small, ill-defined peak in the Hg (0) reoxidation region, around 0.6 V. The peak current associated to this latter signal was only a few percent (ca. 4 %) of the initial signal recorded at Day #0, suggesting a strong evolution of the GC/AuNPs interface structure and probably a loss of gold material. No peak was further observed after Day #7 on GC/AuNPs. On the contrary, on $GC/SH_{(CPE)}/AuNPs_{(CPE)}$ (Figure 5B), a clear signal associated to Hg(0) reoxidation was observed for a much longer time. At Day #0, the SWASV exhibited a shape comparable to that recorded on GC/AuNPs, with two peaks located at 0.25 V and 0.49 V and associated to chloride anions desorption and Hg(0) reoxidation, respectively. The slight difference noticed in peak potential values may be accounted for considering the presence of the organic film. After 7 days of storage, a clear reoxidation signal located at 0.54 V was still observed. The corresponding peak current was around 13 % of the initial signal recorded at Day #0. After 21 days of storage, the signal at 0.54 V was still present on the SWASV, the corresponding peak current being around 6 % of the initial signal recorded on $GC/SH_{(CPE)}/AuNPs_{(CPE)}$. This

latter result shows that Hg(II) trace determination would be possible using a GC/$SH_{(CPE)}$/$AuNPs_{(CPE)}$ electrode even after three weeks. Figure 5C depicts the evolution of the peak current corresponding to a 4 nM Hg(II) concentration recorded by SWASV in a 0.01 M HCl solution as a function of storage time over a four-week period. The response obtained on GC/$SH_{(CPE)}$/$AuNPs_{(CPE)}$ electrodes strongly decreased during the first days to reach 13 % of initial signal recovery after one week. Then, the decrease in the response diminished, and around 6 % of the initial signal was still measured after three weeks. It is worth noting that although very small (ca. 14 nA), the corresponding signal clearly differentiated from the background, proving the sensor to be actually still sensitive. After a storage of four weeks, a signal was still recorded, but the repeatability was very poor and the corresponding value has to be considered an outlier. GC/AuNPs electrodes exhibited a faster decrease in signal recovery, since only 4 % of the initial signal was recorded after one week, ie more than three times lower than for GC/SH/AuNPs electrodes. No more signal was recorded after a storage of eight days. Thus, the presence of the organic film bearing SH group significantly enhanced the stability of the mixed diazonium/AuNPs interface, and thus the sensor lifetime.

In conclusion, efficient AuNPs electrodeposition on thick (ca. 4 nm) diazonium film was demonstrated for the first time. One may assume Au(III) reduction to proceed initially via the pinholes present in the organic film. Once the first nuclei are generated, electron transfer throughout the film is restored, and a classical nucleation/growth pathway occurs. The blocking effect of the diazonium film is also probably in part counterbalanced by the affinity of Sulphur atoms for Au, which may favor metal cations approach. The as-prepared AuNPs were proved to be sensitive towards Hg (II) trace determination. Moreover, the mixed organic/inorganic interface was found to significantly enhance the sensor lifetime. Once again, this may be due to the strong affinity of Sulphur atoms for Au, which may help at AuNPs stabilization. These results open the way to long-term deployment in natural media of sensors dedicated to trace metal elements determination.

Experimental Section

All chemicals were of analytical grade and used as received. 4-thiophenol diazonium synthesis was conducted according to a previously published procedure [8].

Electrochemical experiments were performed using a Metrohm Autolab PGSTAT 128 N potentiostat interfaced to a personal computer and controlled with NOVA 2.1 software package. A classical water-jacketed three-electrode glass cell was used with a Metrohm platinum rod and a Radiometer saturated calomel electrode (SCE) isolated from the solution by a glass frit as counter and reference electrodes, respectively. Working electrode was a 3 mm diameter glassy carbon (GC) rotating disk electrode from Radiometer or a pyrolyzed photoresist film (PPF) plate (6 mm diameter) prepared at the Institut des Sciences Chimiques de Rennes according to published procedure [14].

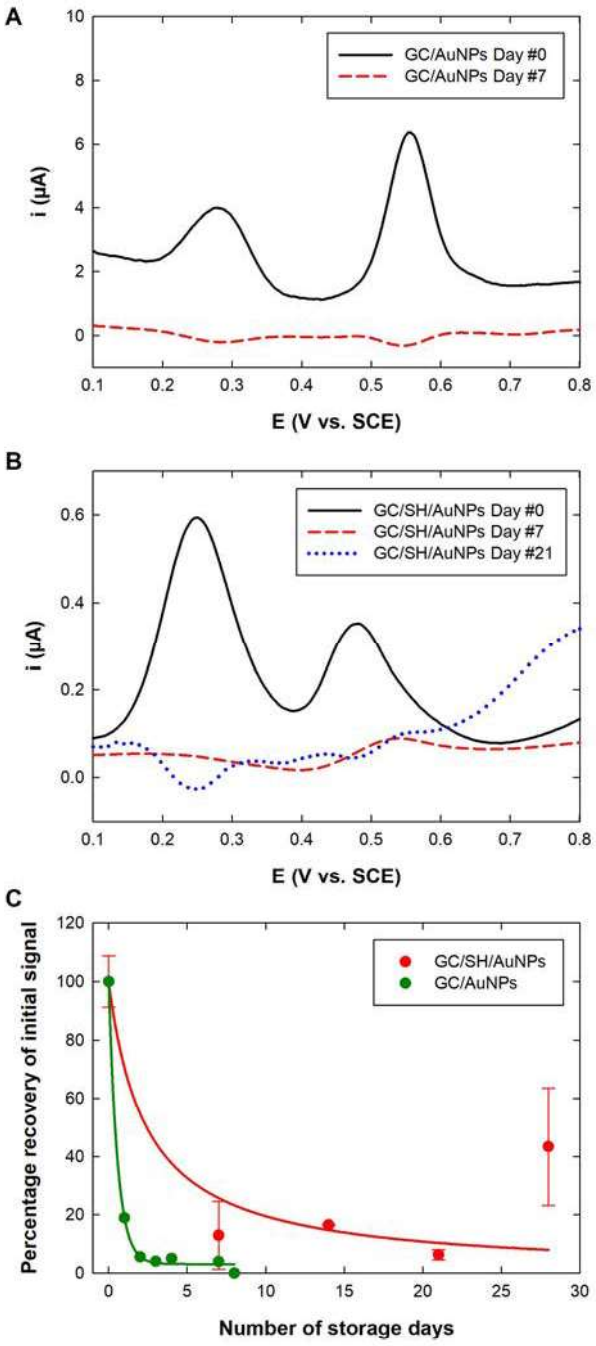

Fig. 5. SWASVs recorded in a 0.01 M HCl solution containing 4 nM Hg(II) on (A) GC/AuNPs and (B) GC/$SH_{(CPE)}$/$AuNPs_{(CPE)}$ for different storage durations. (C) Evolution of the peak current corresponding to Hg(0) reoxidation on the SWASVs for a 4 nM Hg(II) concentration versus time recorded on (red) GC/$SH_{(CPE)}$/$AuNPs_{(CPE)}$ and (green) GC/AuNPs electrode. Each measurement was conducted 4 times. Between each measurement, the electrodes were left in air.

Atomic force microscopy (AFM) images w ere recorded at the Institut des Technologies Avancées en Sciences du Vivant (ITAV) using a JPK NanoWizard II running a Bruker MSNL– E probe in contact mode on the PPF plate. Field emission gun scanning electron microscopy (FEG-SEM) w as performed at the Atelier Interuniversitaire de Micro-nano Électronique (AIME) using a JEOL JSM 7800F w ith accelerating voltage of 8 kV. Image processing (particles density and average diameter determination) w as achieved using a homemade MATLAB program [6–8, 15].

Hg(II) detection w as performed using a previously reported square w ave anodic stripping voltammetry (SWASV) procedure [7].

Acknowledgements

This work was supported by the French Agence Nationale de la Recherche as part of the MERcury Electrochemical SENSor for in situ trace determination (MERESENS) project (ANR-15-CE04-0010).

References

[1] S. P. Roy, *Ecoscan* **2010**, *4*, 235–240.

[2] L. Järup, *Br. Med. Bull.* **2003**, *68*, 167–182.

[3] D. Omanović, C. Garnier, K. Gibbon-Walsh, I. Pižeta, *Electrochem. Commun.* **2015**, *61*, 78–83.

[4] a) E. E. L. Tanner, R. G. Compton, *Electroanalysis* **2018**, *30*, 1336–1341; b) G. March, T. D. Nguyen, B. Piro, *Biosensors* **2015**, *5*, 241–275.

[5] A. Chen, B. Shah, *Anal. Methods* **2013**, *5*, 2158–2173.

[6] a) T. Hezard, K. Fajerwerg, D. Evrard, V. Colliere, P. Behra, P. Gros, *J. Electroanal. Chem.* **2012**, *664*, 46–52; b) T. Hezard, K. Fajerwerg, D. Evrard, V. Colliere, P. Behra, P. Gros, *Electrochim. Acta* **2012**, *73*, 15–22.

[7] L. Laffont, T. Hezard, P. Gros, L.-E. Heimbürger, J. E. Sonke, P. Behra, D. Evrard, *Talanta* **2015**, *141*, 26–32.

[8] E. Gervais, Y. Aceta, P. Gros, D. Evrard, *Electrochim. Acta* **2018**, *261*, 346–355.

[9] a) D.-j. Guo, H.-l. Li, *Electrochem. Commun.* **2004**, *6*, 999–1003; b) D. J. Guo, H. L. Li, *Carbon* **2005**, *43*, 1259–1264.

[10] G. Liu, Y. Zhan, W. Guo, *Biosens. Bioelectron.* **2014**, *61*, 547–553.

[11] F. Mirkhalaf, K. Tammeveski, D. J. Schiffrin, *Phys. Chem. Chem. Phys.* **2009**, *11*, 3463–3471.

[12] a) M. C. R. González, A. G. Orive, R. C. Salvarezza, A. H. Creus, *Phys. Chem. Chem. Phys.* **2016**, *18*, 1953–1960; b) M. C. R. González, L. M. Rivera, E. Pastor, A. H. Creus, G. García, *J. Catal.* **2018**, *366*, 1–7.

[13] a) A. J. Downard, *Langmuir* **2000**, *16*, 9680–9682; b) A. J. Downard, M. J. Prince, *Langmuir* **2001**, *17*, 5581–5586.

[14] a) S. Ranganathan, R. McCreery, S. M. Majji, M. Madou, *J. Electrochem. Soc.* **2000**, *147*, 277–282; b) L. Lee, Y. R. Leroux, P. Hapiot, A. J. Downard, *Langmuir* **2015**, *31*, 5071–5077.

[15] E. Granado, E. Gervais, G. Gotti, S. Desclaux, M. Meireles, P. Gros, D. Evrard, *Int. J. Electrochem. Sci.* **2017**, *12*, 6092–6107.

[16] a) C. Saby, B. Ortiz, G. Y. Champagne, D. Belanger, *Langmuir* **1997**, *13*, 6805–6813; b) S. Baranton, D. Belanger, *J. Phys. Chem. B* **2005**, *109*, 24401–24410; c) S. S. C. Yu, A. J. Downard, *e-J. Surf. Sci. Nanotechnol.* **2005**, *3*, 294–298; d) A. Omrani, A. A. Rostami, N. Yazdizadeh, M. Khoshroo, *Chem. Phys. Lett.* **2012**, *539–540*, 107–111.

[17] a) G. Gunawardena, G. Hills, I. Montenegro, B. Scharifker, *J. Electroanal. Chem.* **1982**, *138*, 225–239; b) D. Grujicic, B. Pesic, *Electrochim. Acta* **2002**, *47*, 2901–2912.

[18] J.-M. Noël, B. Sjöberg, R. Marsac, D. Zigah, J.-F. Bergamini, A. Wang, S. Rigaut, P. Hapiot, C. Lagrost, *Langmuir* **2009**, *25*, 12742–12749.

[19] T. Hezard, L. Laffont, P. Gros, P. Behra, D. Evrard, *J. Electroanal. Chem.* **2013**, *697*, 28–31.